IJE TRANSACTIONS B: Applications Vol. 36, No. 08, (August 2023) 1520-1531

International Journal of Engineering

Journal Homepage: www.ije.ir

Energy Management of an Integrated PV/Battery/Electric Vehicles Energy System Interfaced by a Multi-port Converter

P. Tarassodi[a], J. Adabi*[a], M. Rezanejad[b]

[a] *Faculty of Electrical and Computer Engineering, Babol Noshirvani University of Technology, Babol, Iran*
[b] *Faculty of Engineering and Technology, University of Mazandaran, Babolsar, Iran*

PAPER INFO

Paper history:
Received 7 April 2023
Received in revised form 22May 2023
Accepted 24 May 2023

Keywords:
Energy Mannagement
Multiport Converter
Electric Vehice
Photovoltaic System

ABSTRACT

Integrated energy systems, including renewable energy sources (RES) and battery energy storage (BES), have high potentialities to deal with issues caused by the high penetration of electric vehicles (EVs) in power systems. The full realization of the benefits of such systems depends on implementation of an energy management system (EMS) in order to monitor power sharing between different components of the system. In this paper, an EMS is proposed for a multi-port converter as an integrated PV/BES/EV energy system. It takes into account the EV mileage, BES dis/charge cycles and financial benefits, and schedule for the optimal dis/charge of batteries, and also involves EVs in V2X programs. In this approach, the potential of EVs as a portable energy storage can be employed in providing ancillary services to the power grid. The obvious advantages of the proposed EMS performance have been specified by simulation and comparison with the benchmark method. According to the obtained results, for a specific period of time, a better interaction has been established between the average achievement of the final SOC and the financial profit of the integrated energy system under the proposed EMS. According to the proposed method, for a 10% reduction in the final SOC compared to the benchmark method, the minimum financial benefit is about 0.2607 pounds (received from the grid), equivalent to 0.2082 pounds (paid to the grid) in the benchmark method.

doi: *10.5829/ije.2023.36.08b.12*

1. INTRODUCTION

In past decades, the tendency to use RES in power systems has increased as a promising solution to deal with environmental, technical and economic challenges. Concerns regarding the reliability of their operation have also increased. One solution is the integration of RES with BES, which result in financial benefits from the sale of excess power [1]. Such systems also play a significant role in supporting the power grid. For instance, with the increasing penetration of EV, providing charging points based on integrated energy systems is considered a suitable solution to avoid problems caused by the increase in power grid load demand. Such that it provides a clean charging point, without applying an additional load on the power grid. Integrated energy systems are created by combining different sources such as RES, BES, EV and Grid with power electronic interfaces that exchange power under the supervision of a control system to achieve technical and financial objectives.

So far, various researches have investigated several aspects of the implementation of integrated energy systems and their performance. An EMS strategy based on particle swarm optimization (PSO) and fuzzy controller for a microgrid consisting of distributed generation resources and energy storage system consisting of batteries and supercapacitors are proposed by Sepehrzad et al. [2]. A family of multifunctional multi-port converters suitable for PV-based EV charging stations and grid-connected BES is introduced and simulated by Gohari et al. [3]. Active and reactive exchange power control is carried out by two-loop PI control scheme in this structure. Moreover, a rule-based EMS is presented to improve system reliability at a

*Corresponding Author Email: j.adabi@nit.ac.ir (J. Adabi)

Please cite this article as: P. Tarassodi, J. Adabi, M. Rezanejad, Energy Management of an Integrated PV/Battery/Electric Vehicles Energy System Interfaced by a Multi-port Converter, ***International Journal of Engineering, Transactions B: Applications***, Vol. 36, No. 08, (2023), 1520-1531

reduced cost. A dis/charging scheduling algorithm based on a chance constrained programming method for an EV charging station including BES and PV is proposed by Li et al. [4]. In the proposed algorithm, EV dis/charging is influenced by PV uncertainty, dis/ charging priorities and electricity price, and it's able to reduce energy costs by 50%. A practical test of a smart charging controller based on PSO-ANN-Fuzzy is conducted by Ali et al. [5], which considers user needs, energy tariff, grid conditions (for example, voltage or frequency), renewable (PV) output, and battery's state of health (SOH) status. The intended structure has RES and BES and is connected to the three-phase power grid from one side. A topology for a multi-port DC/DC/AC converter, suitable for use in BES-based hybrid microgrids is proposed by Zhang et al. [6]. Also, a detailed description of the control system and decentralized power management of the proposed structure has been discussed. A multi-mode hierarchical power management strategy for a smart home as a nine-port energy router is proposed by Wang et al. [7]. Nine-ports have been provided through separate conventional converters. The proposed strategy is based on droop and three-mode switching relationships to ensure the power balance of the entire system, which sends the current references to the decentralized controller. In the controller module, the power sharing of scattered productions is realized in order to support the voltage and frequency of the power system. A smart charging approach for off-grid electric chargers in home applications including PV, BES, and EV is proposed by Gholinejad et al. [8]. The optimal charging profile of BES and EV is carried out through Bellman-Ford-Moor algorithm, in which the financial benefits of EV and home owners have been fulfilled by considering their comfort level. A new interface topology is created by Savrun et al. [9] by combining several existing topologies to integrate two EVs with home DC microgrids. The proposed power management algorithm in this reference is rule-based that determines the state of power flow between the elements of this structure. Its control system is also based on voltage loops that stabilize voltage of the ports on their reference values. A new multiport converter for use in systems with storage is proposed by Yi et al. [10]. In this topology, two active switches are used to provide two bidirectional ports and one unidirectional DC/DC port. A new structure for connecting BESs, EVs and RES is investigated by Engelhardt et al. [11], in which a set of strings is employed instead of the power electronic interface. The proposed EMS for this structure assigns an appropriate string for two fast charging points of EVs according to the PV and SOC production power of BESs. An EMS for a grid-connected charging station is proposed by Mumtaz et al. [12], which is capable of simultaneous scheduling of dis/charging of five different EVs. The proposed algorithm makes it possible to implement V2X and X2V scenarios including 7 different operational modes. The adaptive PID control schematic has been employed to control converters of this system.

To sum up, Table 1 compares the major features in existing researches with those of presented in this article where the relevant researches can be categorized into three general types: power electronics interface topology [3, 6], control systems [9, 12] and EMS strategies [2, 4, 5, 7, 8, 10, 11]. In general, it has been observed that in some of these papers, EMS strategies and control schematics have not been verified through experimental tests. In some studies, the description of power electronic converters as integral components of integrated energy systems has not been addressed. Also, the researches that focused on topology are different from each other in terms of the number of bidirectional ports and simultaneous availability of DC and AC ports. In addition, in some works, control of voltage and current of sources has been neglected, while without an efficient control system, power sharing between different sources will not be possible. Battery dis/charging plans are often aimed at power balance, and the lack of short and long-term EMS is clearly felt considering electricity purchase and sale tariffs. The performance of integrated energy systems, to a large extent, depends on the EMS strategy, because it's responsible for scheduling, monitoring and controlling power exchanges between different components of the system [11]. The objectives of EMS strategies include charging BES through excess power [13], minimizing energy costs [1, 4, 8], reducing grid pressure [12], and also reducing system losses [14, 15]. Thus, the main focus here is on presenting an EMS strategy for an integrated energy system, which aims to reduce energy costs and facilitate EV participation in V2X programs, as a potential energy source. Also, the maximum energy that can be stored in batteries (BES and EV), based on the battery health curve-the number of dis/charge cycles, is included in the proposed EMS. In this way, the gradual effect of battery degradation on EMS scheduling can be investigated. However, in order to set up and examine the overall performance of such a system, aspects of the topology of the power electronics interface and its control system have also been discussed. In general, the major contributions of this paper are stated below:

- Proposing an EMS based on mathematical relations with easy implementation
- Integrated MIMO converter control
- Facilitating EV connection/disconnection to/from EMS and Reducing energy price of EV charging
- Facilitating use of EV in V2X programs and Considering SOH of batteries in EMS based on dis/charge number

This paper is organized as follows: description of the MIMO converter topology and control schematic is provided in the second part. The relations and flowchart

of the proposed method are presented in the third part. The third section includes the system model, how to apply restrictions and process of EMS. The fourth part examines and discusses the simulation results. In the end, a summary and results of the study are presented in conclusion in the fifth section. The novelty of this paper lies in the development of a power electronic-based control algorithm for power flow management in a grid-connected PV/BES/EV energy systems. This algorithm dynamically allocates power based on real-time energy generation, consumption, and EV charging requirements as well as aiming to maximize overall financial benefits of the system and considering battery degradation. By referring to Table 1, it is evident that there is a clear lack of studies addressing all major aspects of EMS implementation. In addition, different mannagment scenarios of such system was investigated [16-21].

2. SYSTEM DESCRIPTION

The general schematic of the integrated energy system is displayed in Figure 1. This system has three parts: Power electronics interface converter, control system and EMS. The power electronics interface is a MIMO converter that has two bidirectional DC/DC ports, one unidirectional DC/DC port and one bidirectional AC/DC port. This converter provides the possibility of power exchange between PV, EV, BES and the power grid under a fewer number of switches. So, compared to topologies with similar capabilities, two less switches are used in its structure. The MIMO converter consists of connecting two DC/DC and DC/AC sections; in the first section, dis/charging of batteries is provided through the DC-link or through each other. In the second part, it's possible to inject power from the DC-link to the power grid, from the power grid to the DC-link, and from PV to the DC-link. In this way, power exchanges in this topology can be conducted with different objectives, including sharing PV and BES for EV charging and reducing power grid stress. Moreover, this system provides the possibility of dis/charging BES and EV to achieve financial benefits and participate in V2X applications.

In a recent study conducted by Tarassodi et al. [22], performance of the integrated energy system under the above-mentioned topology has been thoroughly

TABLE 1. Comparison table for existing studies

Ref	Sources	Power electronics		Controller system			EMS constrains		
		No. of Bidirectional Ports	No. of switches	Constant power	Constant voltage	V2X	Battery degradation	Tariff	EV revenue
[1]	Grid, BES, EV, PV, CHP	2 DC, 1 AC	9	✓	✓	V2G, V2BES	×	MCP	×
[3]	Grid, BES, EV, PV	1 DC, 1 AC	7	✓	✓	×	×	×	×
[4]	Grid, BES, EV, PV	-	-	×	×	V2G	✓	MCP	✓
[5]	Grid, BES, EV, PV	-	-	×	×	V2G, V2BES	✓	MCP	✓
[6]	AC and DC Grids, BES	3 DC, 1 AC	9	✓	✓	×	×	×	×
[7]	Hybrid AC/DC microgrid	1 DC, 1 AC	23	✓	✓	×	×	×	×
[8]	Grid, BES, EV, PV	2 DC, 1 AC	9	✓	✓	V2G, V2BES	×	MCP	×
[9]	EV	1 DC	9	✓	✓	V2H	×	×	×
[10]	BES, EV, PV	1 DC	2	×	×	×	×	×	×
[13]	Grid, BES, PV	1 DC, 1 AC	9	✓	✓	×	×	×	×
[16]	Grid, BES, PV	×	×	×	×	×	✓	MCP and FIT	×
[17]	Grid, BES, PV	1 DC, 1 AC	8	✓	✓	×	×	×	×
[18]	Grid, EV, PV	1 AC	15	✓	✓	×	×	×	×
[19]	Grid, BES	1 DC, 1 AC	14	✓	✓	×	×	×	×
[20]	Grid, BES, PV, Fuel cell	1 DC	14	✓	✓	×	×	×	×
[21]	DC source, Super capacitor	×	6	✓	✓	×	×	×	×
Proposed	Grid, BES, EV, PV	2 DC, 1 AC	9	✓	✓	V2G, V2BES	✓	MCP and FIT	✓

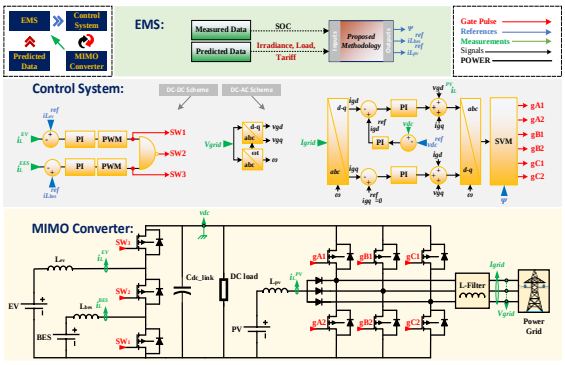

Figure 1. General view of integrated energy system

investigated. With continuous sampling of voltage of the power grid and DC-link as well as current of the inductors, the control system stabilizes values of these quantities on the determined references. The control schematics of DC/DC and DC/AC sections are separated in Figure 1. The control system in DC/DC section includes current loops that apply error of the inductor current to PWM unit after passing through the PI regulator. In this way, switching pulse of SW_1 and SW_3 switches are generated. Also, the switching signal of SW_2 switch is obtained with NAND of two SW_1 and SW_3 signals. In this schematic, the current reference values iL_{EV}^{ref} and iL_{BES}^{ref} are determined by EMS, as discussed in the next section. In the DC/AC control schematic, by using a voltage loop, the voltage error of DC-link is passed through a PI regulator to obtain the value of the direct component of the inverter current reference. This value determines the amount of power that must be exchanged by the inverter to stabilize DC-link voltage at the specified reference value.

In this schematic, the space vector modulation (SVM) method is applied so that in addition to its inherent advantages, PV system integrated with the three-phase, three-leg inverter can be controlled. In this way, one less switch is used in MIMO converter. In order to control PV, the application of ψ parameter to SVM algorithm is used to change the duration of vector [1,1,1] in SVM according to the environmental conditions such as the intensity of radiation and temperature. Because under the other seven vectors, the PV inductor is only charged and as long as vector [1,1,1] is applied, the energy stored in PV inductor is discharged in DC-link capacitor. Although there are some challenges in implementation of such an integrated control system, this paper focuses on EMS, as described in detail in the next section.

3. METHODOLOGY

In this section, the proposed method of this paper is described in how to share resources to gain financial and technical benefits. To begin with, Equation (1) represents the power balance in MIMO converter, in which PV generated power (P_{PV}), BES power in discharge mode (P_{BES}^{DisCh}) and EV power in discharge mode (P_{EV}^{DisCh}) are considered positive. In contrast, BES power in charging mode, EV power in charging mode and load power are considered negative. As a result, the positive value of P_{Grid} is indicative of the injection of excess power of the integrated energy system towards the power grid and vice versa.

$$P_{Grid} = P_{PV} + P_{BES}^{DisCh} + P_{EV}^{DisCh} - P_{BES}^{Ch} - P_{EV}^{Ch} - P_{LOAD} \quad (1)$$

where the amount of load consumption power (P_{LOAD}) is considered available and definite for the day-ahead. Also, P_{PV} is calculated according to the radiation intensity profile, which normally starts from zero and reaches maximum value from early morning to noon. Then, it gradually reaches zero until night. Here, the radiation intensity is considered definite and predetermined; however, to achieve the maximum power point (MPP) for changes in the radiation intensity, the PV system is modeled further. Equation (2) analytically expresses the I-V characteristic of the solar cell [23]. In this model, effect of the resistance of series and parallel branches in the solar cell model is addressed. Despite the existence of more accurate models, this model establishes an interaction between accuracy and simplicity [24, 25].

$$I = N_p I_{pv,cell} - N_p I_{0,cell}\left[exp\left(\frac{q(V+R_s I_{0,cell})}{N_s akT}\right) - 1\right] - \frac{V+R_s I_{0,cell}}{R_p} \quad (2)$$

where, q is the charge of an electron (Coulomb), k is Boltzmann's constant (J/K), T is the temperature of the p-n junction (K), a is the ideality constant of the diode, N_p is the number of parallel cells, N_s is the number of series cells, R_s is the equivalent series resistance and R_p is the equivalent parallel resistance. Also, $I_{0,\,cell}$ is the reverse saturation current of the diode [23]:

$$I_{0,cell} = \frac{I_{sc,n}+K_I\Delta T}{exp\left(\frac{q(V_{oc,n}+K_V\Delta T)}{(N_s akT)}\right)-1} \quad (3)$$

in which, K_V is the voltage coefficient, $I_{sc,n}$ is the short circuit current and $V_{oc,n}$ is the open circuit voltage of the cell under nominal conditions. $I_{pv,\,cell}$ is the production current of a cell, which has a direct relationship with the intensity of radiation and temperature. Equation (4) describes the mathematical description of the impact of intensity of radiation and temperature on this parameter.

$$I_{pv,cell} = \left(I_{pv,n} + K_I\Delta T\right)\frac{G}{G_n} \quad (4)$$

where, K_I is the current coefficient, G_n is the nominal radiation amount (W/m^2), the difference between the ambient temperature and nominal condition temperature (Kelvin) and $I_{pv,n}$ is the nominal current of the cell under nominal conditions. By specifying the current value, the

PV output voltage value is also obtained from the I-V curve. Multiplying voltage and current of PV has only one maximum point, which may not be on the MPP due to the environmental conditions. To this end, the perturb and observe (P&O) algorithm is used for MPPT in PV model, and Algorithm 1 represents the pseudo code of its modelling [23]. In this algorithm, the applied signal ψ is generated by SVM method instead of calculating duty cycle of the switches.

Algorithm 1. MPPT Algorithm

```
//Input: Instantaneous current, Instantaneous voltage, Ψ(0)=0.
Calculate instantaneous power:
 if (p_pv(t)> p_pv(t-1))
        if (v(t)> v(t-1))
            Ψ(t) = Ψ(t-1) + Δ Ψ;  // Δ Ψ ≈ 1μs
        else
            Ψ(t) = Ψ(t-1) - Δ Ψ;
        end
 elseif ((p_pv(t)< p_pv(t-1))
        if (v(t)> v(t-1))
            Ψ(t) = Ψ(t-1) - Δ Ψ;
        else
            Ψ(t) = Ψ(t-1) + Δ Ψ;
        end
 else
            Ψ(t)= Ψ(t-1);
 end
//Output: Ψ(t).
```

In this way, by calculating PV generated power and the availability of load consumption power, only by determining BES and EV charging and discharging power values by EMS, it's possible to determine the exchanged power value of the energy system integrated with the power grid. For this purpose, first, the standard discrete time model of the battery is placed in the power balance relation. Then, in each time step, for different values of BES and EV power, the minimum amount of energy cost or maximum financial benefit of the integrated energy system is calculated based on purchase/sale tariff values. Thus, the P_{Grid} value for the next time step is determined. The discrete time model of the stored energy of the battery is shown in Equation (5), in which E[k] is the energy stored in the battery at the instant of $k \in \tau = \{0, 1, \ldots, T\text{-}1\}$6. Moreover, η_{Ch} and η_{DisCh} are charge and discharge efficiency of the battery, respectively, and $P_{Ch}[k]$ and $P_{DisCh}[k]$ are charge and discharge power of the battery in k^{th} time step, respectively, and $\Delta t>0$ indicate one time step length [26].

$$E[k+1] = E[k] + \eta_{Ch}\Delta t P_{Ch}[k] - \frac{\Delta t}{\eta_{DisCh}} P_{DisCh}[k], \forall k \in \tau \quad (5)$$

The constraints of the problem for $\forall k \in \tau$ are also given in Equations (6) to (10). The set of Equations (5) to (10) has been used to model BES and EV, with the difference that initial and nominal energy values, maximum dis/charging power, as well as charging and discharging efficiency of BES and EV are considered differently [26-30].

$$E[0] = E_0 \quad (6)$$

$$0 \le P_{Ch}[k] \le P_{Ch}^{max} \quad (7)$$

$$0 \le P_{DisCh}[k] \le P_{DisCh}^{max} \quad (8)$$

$$0 \le E[k+1] \le E_{max} \quad (9)$$

$$P_{Ch}[k]P_{DisCh}[k] = 0 \quad (10)$$

Equation (10) models the condition of complementarity of battery charging and discharging, which proves that a battery cannot be charged and discharged simultaneously. This equality has created a non-linear term in energy management calculations, which challenges the solution of such problems. Therefore, Equation (5) will become Equation (11) by removing restriction (10) and simplifying.

$$E[k+1] = E[k] + \eta\Delta t P_{Bat}[k], \qquad \forall k \in \tau \quad (11)$$

$$-P_{CH}^{max} \le P_{Bat}[k] \le P_{DisCh}^{max} \quad (12)$$

In Equation (11), an input ($P_{Bat}[k]$) is considered to calculate battery energy, defined as follows:

$$P_{Bat}[k] = P'_{DisCh}[k] - P'_{Ch}[k], \qquad \forall k \in \tau$$
$$P'_{Ch} = max\{0, -(P_{DisCh} - P_{Ch})\} \quad (13)$$
$$P'_{DisCh} = max\{0, P_{DisCh} - P_{Ch}\}$$

According to Equation (11), for each possible value of E[k+1], a P_{Bat} value is obtained for batteries. Since ΔE changes in each time step is constraint by the inequality (12), for all the values that apply to this inequality, one should look for a P_{Bat} value for BES and EV, so that by placing it in Equation (1), the optimal value of exchanged power between the power grid and the integrated energy system can be obtained. Under the optimal amount of exchanged power, there would be the lowest energy cost, the highest financial profit and the lowest battery degradation. For this reason, after inserting the possible values of E[k+1] and calculating P_{Bat} (for BES and EV separately), taking into account parameters such as electricity purchase/sale tariffs, number of dis/charging cycles, EV mileage and minimum depth of discharge (DOD), the optimal value of exchanged power are obtained. The intended multi-objective function in the proposed EMS is provided in Equation (14). This objective function seeks to increase SOC and simultaneously, increase the financial benefit (reducing the cost paid to the grid or increasing cost received from the grid). For this purpose, in addition to the grid power, the power of the batteries is also multiplied in the purchase and sale tariffs depending on their sign.

$$[P_{Grid}, P_{BES}, P_{BES}, \pi_p, \pi_i] = \begin{cases} if(P_{Grid} \geq 0) \begin{cases} if(P_{BES} \geq 0) \begin{cases} \frac{(P_{BES}+P_{EV})}{P_{Grid}}, if(P_{EV} \geq 0) \\ \frac{(P_{BES}\pi_i+P_{EV}\pi_p)}{P_{Grid}\pi_i}, if(P_{EV} < 0) \end{cases} \\ if(P_{BES} < 0) \begin{cases} \frac{(P_{BES}\pi_p+P_{EV}\pi_i)}{P_{Grid}\pi_i}, if(P_{EV} \geq 0) \\ \frac{(P_{BES}\pi_p+P_{EV}\pi_p)}{P_{Grid}\pi_i}, if(P_{EV} < 0) \end{cases} \end{cases} \\ f(P_{Grid} < 0) \begin{cases} if(P_{BES} \geq 0) \begin{cases} \frac{(P_{BES}\pi_i+P_{EV}\pi_i)}{P_{Grid}\pi_p}, if(P_{EV} \geq 0) \\ \frac{(P_{BES}\pi_i+P_{EV}\pi_p)}{P_{Grid}\pi_p}, if(P_{EV} < 0) \end{cases} \\ if(P_{BES} < 0) \begin{cases} \frac{(P_{BES}\pi_p+P_{EV}\pi_i)}{P_{Grid}\pi_p}, if(P_{EV} \geq 0) \\ \frac{(P_{BES}+P_{EV})}{P_{Grid}}, if(P_{EV} < 0) \end{cases} \end{cases} \end{cases} \quad (14)$$

The electricity purchase/sale tariff information is available for the day-ahead and like PV and load, is considered to be predetermined and definite. The number of dis/charging cycles, as a criterion in determining SOH of the BES battery is applied as a constraint of the problem and overshadows decision-making process in the proposed EMS. For this purpose, the declining curve of the maximum storable energy of BES in terms of changes in number of dis/charging cycles is applied to the problem as an input. The number of dis/charging cycles for a new battery is considered zero. But, for each charge or discharge, its value increases in the proposed algorithm. Moreover, EV mileage is considered as a criterion of its SOH in the proposed EMS. Similarly, the declining curve of SOH with respect to mileage changes is used to limit the problem in terms of the maximum energy that can be stored in EV.

The application of E[k+1] quantification restriction is well shown in Figure 2. As shown in the figure, in k+1 time step, due to an increase in the number of dis/charging cycles or operation compared to before, the final limit of the energy that can be stored in the battery has slightly decreased. Hence, the range of changes of possible value of E[k+1] in k+1 time step has become more limited than before. This would contribute to significant changes in EMS decision-making in the long run. Also, some E[k+1] values are not acceptable. Because in order to achieve these values, the exchanged battery power will exceed the nominal value of condition (12). These values are considered unacceptable and are not considered in the EMS process.

With respect to EV application, in addition to the constraints mentioned in Figure 2, another constraint is applied to E[k+1] value. As it's clear, EV initially behaved as a consumer that needs charging at various home, fast and ultra-fast levels. Depending on the conditions of the integrated energy system, power grid and electricity tariff, one of the above-mentioned charging levels is selected. Anyway, EV working mode is X2V; While based on the objectives of this paper, it may also be used in V2X applications if the EV owner approves. In this case, in X2V mode, E[k+1] quantification takes place only for $\forall k \in \tau \rightarrow E[k] \leq E[k+1]$. In other words, the inequality (12) will change to expression (15) in X2V program. However, in V2X program, it is conducted according to the explanations of Figure 2.

$$-P_{CH}^{max} \leq P_{EV}[k] \leq 0\,, \quad \forall k \in \tau \quad (15)$$

By calculating the average BES dis/charge times and EV performance in 24 hours, it is possible to determine the effect of battery degradation on power sharing in the long term. Moreover, the proposed EMS seeks to reduce the charging time in attaining higher SOCs (lower DOD), which is restricted by the maximum power that can be transferred to the battery, maximum exchanged power with the power grid, financial benefit and, the costs.

The performance description of the proposed EMS is provided in flowchart of Figure 3, in which N_{Ch}^{BES}, N_{Ch}^{EV}, π_p and π_i are the number of BES dis/charge, number of dis/charging cycles, electricity purchase tariff from the power grid and electricity feed-in-tariff (FIT) to the power grid, respectively. The quantification of $E_{BES}[k+1]$ and $E_{EV}[k+1]$ is carried out from the minimum to maximum value of the inequality (9) under

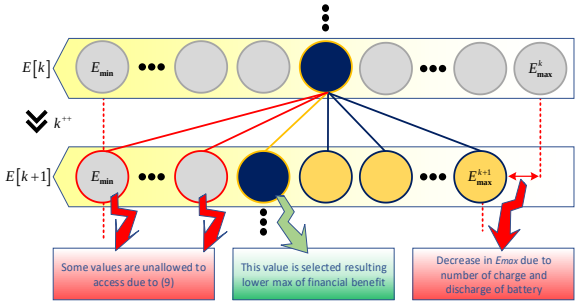

Figure 2. Quantification and restriction of $E[k+1]$

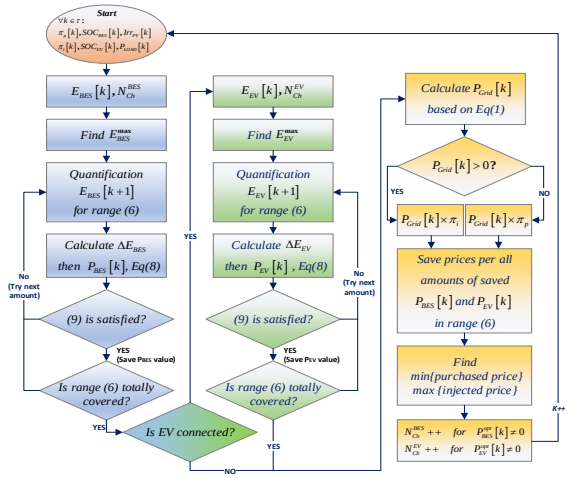

Figure 3. Flowchart of proposed EMS

certain intervals. The maximum value of this inequality is obtained according to N_{Ch}^{BES} and N_{Ch}^{EV} values, based on the battery degradation diagram.

By specifying $P_{EV}[k+1]$, $P_{BES}[k+1]$ and $P_{PV}[k+1]$ values, the MIMO converter is switched under one of the scenarios shown in Figure 4 or a combination of them. As shown, except for part (a), the rest of the scenarios are bidirectional power exchange. Also, it is possible to simultaneously implement one of the scenarios of one part with the scenarios of other parts. For example, PV2DC_{link}, B2V, and G2V scenarios can be simultaneously implemented, which represents EV charging by PV, BES, and the power grid. This means

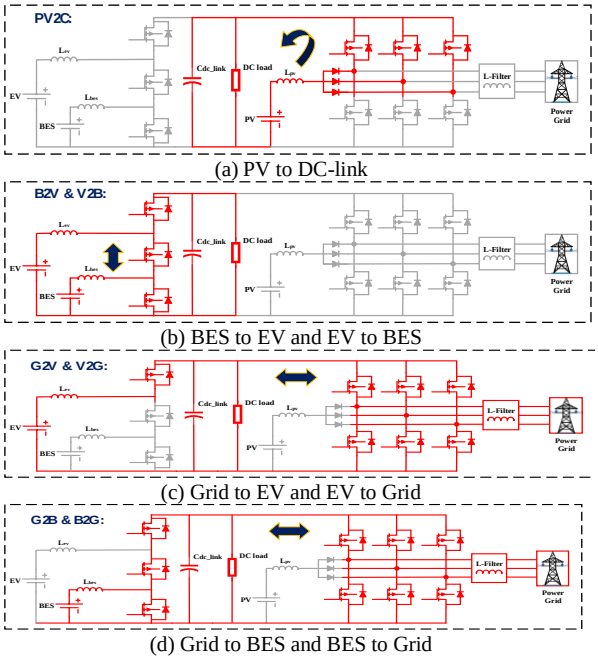

(a) PV to DC-link

(b) BES to EV and EV to BES

(c) Grid to EV and EV to Grid

(d) Grid to BES and BES to Grid

Figure 1. Different operational scenarios of proposed EMS

that the proposed EMS performs both decision-making and determination of power references at the same time. In the previous research conducted by Tarassodi et al. [22], performance of the MIMO converter in terms of the control system, efficiency, reliability, as well as the implementation of different performance scenarios, has been fully investigated and discussed. Therefore, in the next section, only results of the implementation of the proposed EMS on the integrated energy system under study have been examined and compared.

4. RESULTS AND DISCUSSION

In this section, a case study has been simulated in MATLAB, results of which are presented below. Also, in order to check the simulation results, the Simulated Annealing (SA) optimization method has been used as a benchmark. To this end, the SA method has been implemented for a system similar to the proposed method in MATLAB, then the SA analysis has been investigated under the same inputs.

The simulation features of the intended case study are provided in Table 1. The nominal capacity of EV and BES batteries is given in this Table, which by taking into account the EV performance and the number of BES dis/charge cycles**,** determine the maximum energy that can be stored in the batteries. The primary SOC of the batteries is selected as a sample and can change within the permissible range during the planning. The maximum dis/charge power of the batteries are also determined given the capacity of the batteries and MIMO converter. The PV system is also an array of 16 cells connected in series/parallel with the specifications provided in Table 2. Simulation specifications include predicted input data, such as radiation intensity, load consumption power, and electricity tariffs, as shown in Figure 5.

The battery degradation curve is shown in Figure 6. Changes in SOH of BES in relation to an increase in frequency of dis/charging is illustrated in Figure 6(a). As shown in this figure, SOH remains constant until about 100 dis/charge times, then, it gradually reduces. Since the number of EV dis/charge cycles for charging point is not known, the SOH of EV is obtained from Figure 6(b), which is based on mileage changes.

TABLE 2. Simulation parameters value

Description	Value	Unit
Nominal Capacity of BES	1.7	kWh
Nominal Capacity of EV	20	kWh
BES usage	300	Cycle
EV mileage	50000	Miles
BES initial SOC	70	%

EV initial SOC	50	%
BES Dis/Charging power	0.5	kW
EV Dis/Charging power	5	kW
Dis/Charging efficiency	96	%
Lower/upper charge limits	[20-90]	%
Max of irradiance	1000	W/m^2
PV cell current in MPP	7.61	A
PV cell voltage in MPP	26.3	V
Number of PV cells connected in series	8	-
Number of PV cells connected in parallel	2	-

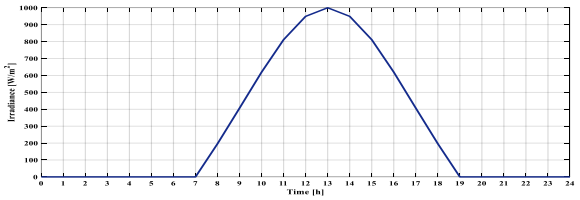

(a) Irradiance

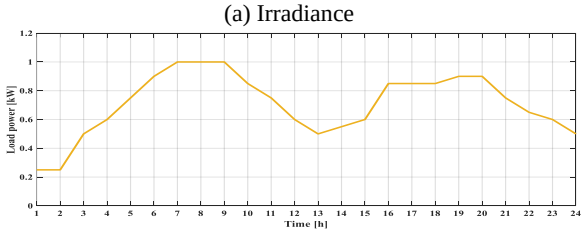

(b) Load power

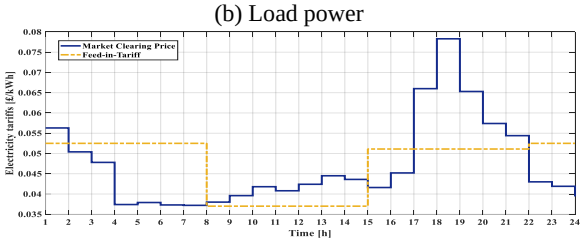

(c) Electricity tariffs

Figure 5. Day-ahead data

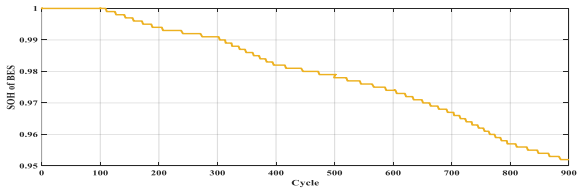

(a) BES

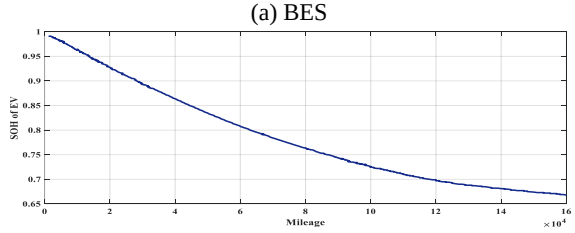

(b) EV

Figure 6. Battery degradation curves

Given the flowchart in Figure 3, with the availability of the predicted inputs as well as measurement of the primary SOC of the batteries, E[k+1] quantification begins. As shown in the explanation of Figure 2, the quantification is conducted under the interval (9) and then, based on conditions such as V2G working mode, the SOH value and the maximum dis/charging power of the batteries would be restricted. Changes in the resource power and SOC of the batteries during 24 hours are shown in Figure 7. These results are achieved under the number of dis/charge cycles of 10 BES and operating range of 1000 miles of EV. In Figure 7(a), the power of the sources that are in the generator state (such as PV and batteries in discharge mode) is positive, and power of the load and batteries in charging mode is negative. As it is shown, with an increase in the PV power, the excess power available in the integrated energy system is used for charging EV. However, in time steps of 14 to 15 (plotted as a column in 15), due to the increase of FIT and increase of EV SOC, not only the EV charging is stopped, but also it is discharged to some extent and the obtained excess power is injected into the power grid. SOC changes of batteries corresponding to paragraph (a) are shown in Figure 7(b). As it's clear in the figure, depending on the conditions of each time step, the batteries are charged or discharged during 24 hours, so that the objective function of the problem is minimized in that time step. Hence, a curve including several charging scenarios and several discharging scenarios has been created.

SOC changes of the batteries under the condition of 300 and 700 cycles, and 50 and 100 thousand miles of operation are illustrated in Figure 8. It is clear in this figure that increasing life of batteries directly affects the integrated energy system planning, such that the dis/charge profile of the batteries has changed compared to before. These changes are more evident in the BES profile, which has a much lower capacity than EV. In the following, the numerical results of these analyses are summarized in Table 2.

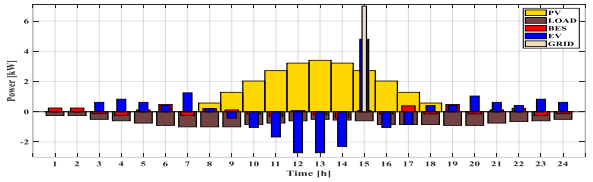

(a) Power of different component

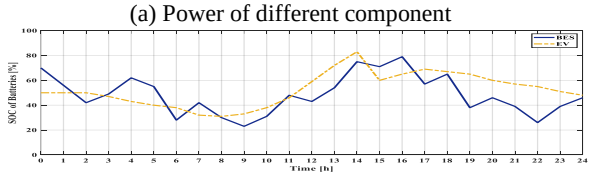

(b) SOC of BES and EV

Figure 7. Changes in power and SOC per cycle=10 & mileage=1000

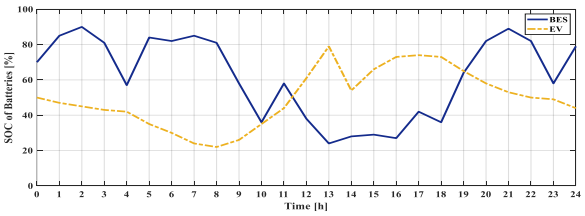

(a) cycle=300 & mileage=50000

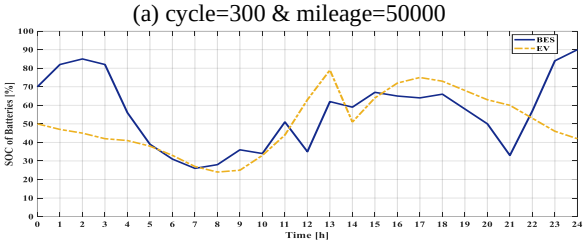

(b) cycle=700 & mileage=100000

Figure 8. SOC of BES and EV under different conditions

On the other hand, increasing EV lifetime, as a high-capacity source, has a greater impact on the amount of EMS income. The 24-hour income of the integrated energy system under cycle and operation changes is shown in Figure 9. It is well known that the increasing EV battery life, as a higher capacity resource, has the greatest impact on the revenue from BES and EV integration in the energy system under study.

Results shown in Figure 10 were obtained under the condition of no EV presence. As it is evident, without the presence of EV, more excess power is available for injection into the power grid. However, the interesting point is that this does not necessarily cause the integrated energy system to achieve higher financial benefits, because it lost the opportunity to benefit from a high-capacity energy storage; and this has reduced the financial benefit of the system for 24 hours. This is because of the fact that FIT is low in the range where more excess power is available. In paragraph (b), SOC BES was obtained under different cycles that did not experience any specific changes without the presence of EV. The numerical results of these analyses are demonstrated in Table 2.

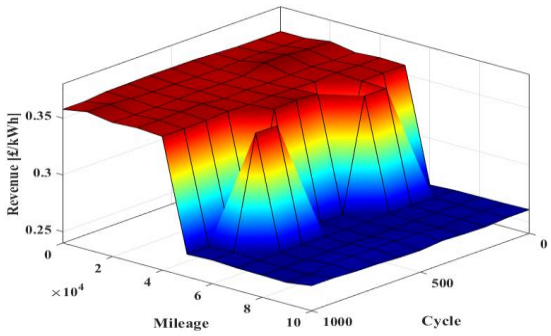

Figure 9. 24-hour energy price per mileage changes

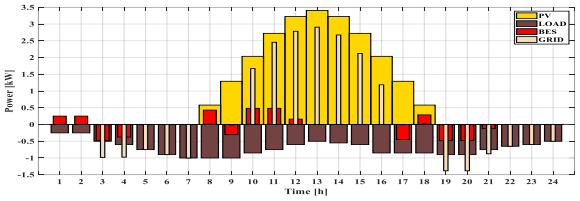

(a) Power of different component

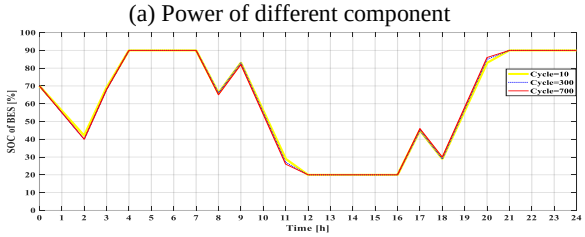

(b) SOC of BES

Figure 10. Changes in power and SOC without EV

The impact of adding EV on the financial benefit of the integrated energy system is shown in Figure 11. This figure proves the effect of the presence of a high-capacity energy storage source (i.e., EV) on the overall financial benefit of the system. Such that in the presence of low-functioning EV, the financial benefit has increased more than 2.3 times compared to the absence of EV. Over time, as the performance of EV increases, this ratio decreases until it reaches 1.6 times per 100,000 miles of operation.

A comparison of the performance of the proposed method with a basic method, namely, SA is illustrated in Figure 12. The time step of this comparison is 1 second and performance of the system under the two proposed and benchmark methods is performed for 86400 seconds.

Results obtained for EV indicate that the final SOC is almost equal, but the dis/charging profile of the batteries under the benchmark method is such that, in total, much less financial benefit is achieved. These results are given in Table 2. So, under the SA method, not only the system has not achieved the financial benefit, but also it has to pay an amount to the power grid. By comparing these results, it's clear that a 10% reduction in SOC in the proposed method is totally acceptable in return for the financial benefit gained. For BES, the newer the batteries are, the greater the final SOC difference under the two

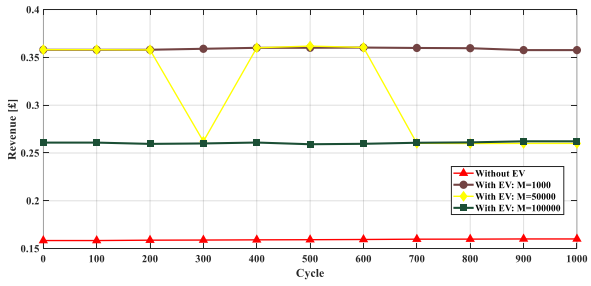

Figure 11. 24-hour energy price per mileage changes, Cycle=0

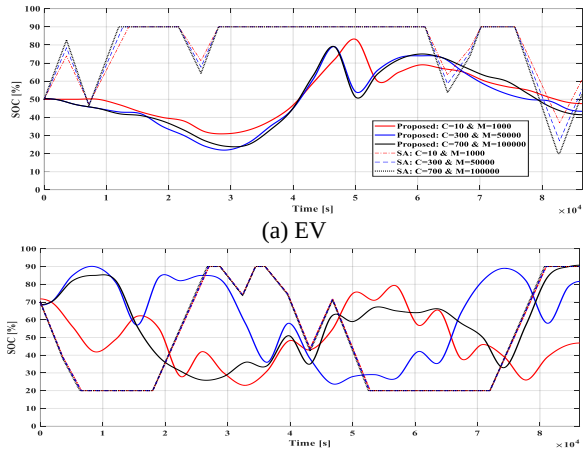

(a) EV

(b) BES

Figure 12. Batteries dis/charging schedule comparison

proposed and SA methods. However, with an increase in lifespan, the final SOC of the batteries has also been obtained similar to each other. In fact, this is a good indication that under the proposed method, an acceptable interaction has been created between the gained financial benefit and the final SOC value of the batteries.

The numerical comparison between the results obtained from the proposed methods and SA, under different cycle and mileage conditions are provided in Table 3. As mentioned in the explanation of the above analysis, the maximum financial benefit under the proposed method is obtained in the presence of EV and SOH above EV.

TABLE 3. Simulation parameters value

Method \ Inputs		Cycle 10	Mileage 1000	Cycle 300	Mileage 50000	Cycle 700	Mileage 100000
Proposed	With EV	0.3580		0.2621		0.2607	
	Without EV	0.1584		0.1589		0.1598	
SA		-0.2979		-0.2344		-0.2082	

5. CONCLUSION

In this paper, an EMS based on mathematical relations is proposed for an integrated PV/BES/EV energy system. The proposed EMS generates BES and EV power references to minimize a multi-objective function, such that it would lead to the reduction of system energy payment costs to the grid and the increase of system costs received from the grid, taking into consideration the final SOC. In the proposed EMS relations, the maximum energy that can be stored in BES and EV are constraint based on the number of dis/charge cycles and mileage, respectively. In this way, an analysis of the effect of increasing the life of batteries and the presence or absence of EV as a high-capacity storage device on the financial benefit is provided. Based on the results obtained from the numerical analysis, it was found that although in the absence of EV, the system sells more energy to the grid, it does not achieve more financial benefits. Because it loses the possibility of using a main source of energy storage in optimal scheduling. Because a significant part of the energy sold was in the absence of EV when FIT is low. On the other hand, in the presence of EV, it is possible to sell significant energy to the grid at high FITs, and the system would achieve a higher financial benefit as a whole.

6. REFERENCES

1. Gholinejad, H.R., Adabi, J. and Marzband, M., "An energy management system structure for neighborhood networks", ***Journal of Building Engineering***, Vol. 41, (2021), 102376. doi: 10.1016/j.jobe.2021.102376.
2. Sepehrzad, R., Moridi, A.R., Hassanzadeh, M.E. and Seifi, A.R., "Intelligent energy management and multi-objective power distribution control in hybrid micro-grids based on the advanced fuzzy-pso method", ***ISA Transactions***, Vol. 112, (2021), 199-213. doi: 10.1016/j.isatra.2020.12.027.
3. Gohari, H.S., Safaeinasab, A. and Abbaszadeh, K., "Family of multifunctional controllable converters for grid, battery, and pv-powered ev charging station applications", in 2022 30th International Conference on Electrical Engineering (ICEE), IEEE. (2022), 681-687.
4. Li, D., Zouma, A., Liao, J.-T. and Yang, H.-T., "An energy management strategy with renewable energy and energy storage system for a large electric vehicle charging station", ***Etransportation***, Vol. 6, (2020), 100076. doi: 10.1016/j.etran.2020.100076.
5. Ali, Z., Putrus, G., Marzband, M., Gholinejad, H.R., Saleem, K. and Subudhi, B., "Multiobjective optimized smart charge controller for electric vehicle applications", ***IEEE Transactions on Industry Applications***, Vol. 58, No. 5, (2022), 5602-5615. doi: 10.1109/TIA.2022.3164999.
6. Zhang, Z., Jin, C., Tang, Y., Dong, C., Lin, P., Mi, Y. and Wang, P., "A modulized three-port interlinking converter for hybrid ac/dc/ds microgrids featured with a decentralized power management strategy", ***IEEE Transactions on Industrial Electronics***, Vol. 68, No. 12, (2020), 12430-12440. doi: 10.1109/TIE.2020.3040660.
7. Wang, R., Jiang, S., Ma, D., Sun, Q., Zhang, H. and Wang, P., "The energy management of multiport energy router in smart home", ***IEEE Transactions on Consumer Electronics***, Vol. 68, No. 4, (2022), 344-353. doi: 10.1109/TCE.2022.3200931.
8. Gholinejad, H.R., Adabi, J. and Marzband, M., "Hierarchical energy management system for home-energy-hubs considering plug-in electric vehicles", ***IEEE Transactions on Industry Applications***, Vol. 58, No. 5, (2022), 5582-5592. doi: 10.1109/TIA.2022.3158352.
9. Savrun, M.M., İnci, M. and Büyük, M., "Design and analysis of a high energy efficient multi-port dc-dc converter interface for fuel cell/battery electric vehicle-to-home (V2H) system", ***Journal of Energy Storage***, Vol. 45, (2022), 103755. doi: 10.1016/j.est.2021.103755.

10. Yi, W., Ma, H., Peng, S., Liu, D., Ali, Z.M., Dampage, U. and Hajjiah, A., "Analysis and implementation of multi-port bidirectional converter for hybrid energy systems", ***Energy Reports***, Vol. 8, (2022), 1538-1549. doi: 10.1016/j.egyr.2021.12.068.
11. Engelhardt, J., Zepter, J.M., Gabderakhmanova, T. and Marinelli, M., "Energy management of a multi-battery system for renewable-based high power ev charging", ***Etransportation***, Vol. 14, (2022), 100198. doi: 10.1016/j.etran.2022.100198.
12. Mumtaz, S., Ali, S., Ahmad, S., Khan, L., Hassan, S.Z. and Kamal, T., "Energy management and control of plug-in hybrid electric vehicle charging stations in a grid-connected hybrid power system", ***Energies***, Vol. 10, No. 11, (2017), 1923. doi: 10.3390/en10111923.
13. Yi, Z., Dong, W. and Etemadi, A.H., "A unified control and power management scheme for pv-battery-based hybrid microgrids for both grid-connected and islanded modes", ***IEEE Transactions on Smart Grid***, Vol. 9, No. 6, (2017), 5975-5985. doi: 10.1109/TSG.2017.2700332.
14. Gamboa, G., Hamilton, C., Kerley, R., Elmes, S., Arias, A., Shen, J. and Batarseh, I., "Control strategy of a multi-port, grid connected, direct-dc pv charging station for plug-in electric vehicles", in 2010 IEEE Energy Conversion Congress and Exposition, IEEE. (2010), 1173-1177.
15. Acha, S., Green, T.C. and Shah, N., "Effects of optimised plug-in hybrid vehicle charging strategies on electric distribution network losses", in IEEE PES T&D 2010, IEEE. (2010), 1-6.
16. Azuatalam, D., Paridari, K., Ma, Y., Förstl, M., Chapman, A.C. and Verbič, G., "Energy management of small-scale pv-battery systems: A systematic review considering practical implementation, computational requirements, quality of input data and battery degradation", ***Renewable and Sustainable Energy Reviews***, Vol. 112, (2019), 555-570. doi: 10.1016/j.rser.2019.06.007.
17. Tang, C.-Y., Chen, P.-T. and Jheng, J.-H., "Bidirectional power flow control and hybrid charging strategies for three-phase pv power and energy storage systems", ***IEEE Transactions on Power Electronics***, Vol. 36, No. 11, (2021), 12710-12720. doi: 10.1109/TPEL.2021.3083366.
18. Kar, R.R. and Wandhare, R.G., "Energy management system for photovoltaic fed hybrid electric vehicle charging stations", in 2021 IEEE 48th Photovoltaic Specialists Conference (PVSC), IEEE. (2021), 2478-2485.
19. Tang, W., Li, Z., Wang, Y., Zhang, C., Shao, L. and Wang, K., "Fpga-based real-time simulation for multiple energy storage systems", in Journal of Physics: Conference Series, IOP Publishing. Vol. 1659, (2020), 012047.
20. Jafari, M., Malekjamshidi, Z., Platt, G., Zhu, J.G. and Dorrell, D.G., "A multi-port converter based renewable energy system for residential consumers of smart grid", in IECON 2015-41st Annual Conference of the IEEE Industrial Electronics Society, IEEE. (2015), 005168-005173.
21. Ahmeti, F. and Arnaudov, D., "Energy flows management of a multi-port dc-dc converter for an energy storage system", in 2022 13th National Conference with International Participation (ELECTRONICA), IEEE. (2022), 1-4.
22. Tarassodi, P., Adabi, J. and Rezanejad, M., "A power management strategy for a grid-connected multi-energy storage resources with a multiport converter", ***International Journal of Circuit Theory and Applications***, https://doi.org/10.1002/cta.3540
23. Gholinejad, H.R., Loni, A., Adabi, J. and Marzband, M., "A hierarchical energy management system for multiple home energy hubs in neighborhood grids", ***Journal of Building Engineering***, Vol. 28, (2020), 101028. doi: 10.1016/j.jobe.2019.101028.
24. Villalva, M.G., Gazoli, J.R. and Ruppert Filho, E., "Comprehensive approach to modeling and simulation of photovoltaic arrays", ***IEEE Transactions on Power Electronics***, Vol. 24, No. 5, (2009), 1198-1208. doi: 10.1109/TPEL.2009.2013862.
25. Carrero, C., Amador, J. and Arnaltes, S., "A single procedure for helping pv designers to select silicon pv modules and evaluate the loss resistances", ***Renewable energy***, Vol. 32, No. 15, (2007), 2579-2589. doi: 10.1016/j.renene.2007.01.001.
26. Nazir, N. and Almassalkhi, M., "Guaranteeing a physically realizable battery dispatch without charge-discharge complementarity constraints", ***IEEE Transactions on Smart Grid***, (2021). doi: 10.1109/TSG.2021.3109805.
27. Sagar, G. and Debela, T., "Implementation of optimal load balancing strategy for hybrid energy management system in dc/ac microgrid with pv and battery storage", ***International Journal of Engineering, Transactions A: Basics*** Vol. 32, No. 10, (2019), 1437-1445. doi: 10.5829/ije.2019.32.10a.13.
28. Basu, A. and Singh, M., "Design and real time digital simulator implementation of a takagi sugeno fuzzy controller for battery management in photovoltaic energy system application", ***International Journal of Engineering, Transactions C: Aspects***, Vol. 35, No. 12, (2022), 2275-2282. doi: 10.5829/ije.2022.35.12c.01.
29. Ahmadigorji, M. and Mehrasa, M., "A robust renewable energy source-oriented strategy for smart charging of plug-in electric vehicles considering diverse uncertainty resources", ***International Journal of Engineering, Transactions A: Basics***, Vol. 36, No. 4, (2023), 709-719. doi: 10.5829/ije.2023.36.04a.10.
30. Ashabi, A., Peiravi, M.M., Nikpendar, P., Salehi Nasab, S. and Jaryani, F., "Optimal sizing of battery energy storage system in commercial buildings utilizing techno-economic analysis", ***International Journal of Engineering, Transactions B: Applications***, Vol. 35, No. 8, (2022), 1662-1673. doi: 10.5829/ije.2022.35.08b.22.

Persian Abstract

چکیده

سیستم‌های انرژی ادغام شده شامل منابع انرژی تجدیدپذیر (RES) و ذخیره‌ساز انرژی باتری (BES)، از پتانسیل بالایی برای مقابله با مشکلات ناشی از نفوذ بالای خودروهای الکتریکی در سیستم‌های قدرت برخودار می‌باشند. تحقق کامل مزایای چنین سیستم‌هایی در گرو پیاده‌سازی یک سیستم مدیریت انرژی (EMS) به منظور نظارت بر اشتراک‌گذاری توان میان اجزای مختلف سیستم می‌باشد. در این مقاله، یک EMS برای یک مبدل چند پورت، به عنوان یک سیستم انرژی ادغام شده PV/BES/EV، پیشنهاد شده است. EMS پیشنهادی، با در نظر گرفتن میزان EV mileage، تعداد شارژ/دشارژ BES و منافع مالی، به برنامه‌ریزی بهینه‌ی شارژ/دشارژ (dis/charging) باتری‌ها پرداخته و EV را در برنامه‌های V2X نیز شرکت می‌دهد. بدین ترتیب، می‌توان از پتانسیل بالقوه‌ی EVها به عنوان یک ذخیره‌ساز پرتابل، در ارائه خدمات جانبی به شبکه قدرت نیز استفاده کرد. مزایای بارز عملکرد EMS پیشنهادی با انجام شبیه‌سازی و مقایسه با روش معیار مشخص شده‌اند. با توجه به نتایج بدست آمده، به ازای یک بازه زمانی مشخص، میان میانگین دستیابی به SOC نهایی و سود مالی سیستم انرژی ادغام شده تحت EMS پیشنهادی تعامل بهتری برقرار شده است. به طوریکه تحت روش پیشنهادی، در ازای ۱۰ درصد کاهش در SOC نهایی نسبت به روش معیار، حداقل منفعی مالی حدود 0.2607 پوند (دریافتی از شبکه) بدست آمده که معادل آن در روش معیار 0.2082- پوند (پرداختی به شبکه) می‌باشد.